First-principles study of the effect of lattice vibrations on Cu nucleation free energy in Fe-Cu alloys

Koretaka Yuge, Atsuto Seko, and Isao Tanaka
Department of Materials Science and Engineering, Kyoto University, Japan

Shigeto R. Nishitani
Department of Informatics, Kwansei Gakuin University, Japan
(Received 23 April 2005; revised manuscript received 8 August 2005; published 1 November 2005)

The effects of lattice vibration on Cu nucleation in Fe-Cu alloys have been investigated by a first-principles technique. We find that the vibrational effect is comparable ($\sim 36\%$) to the configurational entropy. Lattice vibration increases the activation barrier of Cu precipitates by 0.53 eV, where the resulting activation barrier is estimated to be 0.62 eV at critical number n^* of 12 atoms, which is in satisfactory agreement with the previous experimental prediction. Within the description of classical treatment, this increase is interpreted in terms of the associated decrease of driving force due to lattice vibration.

I. INTRODUCTION

Nucleation plays a significant role in the early stage of the structural growth, and it is required to understand and control the formation of nanoscale structures. For accurate prediction of nucleation and its growth, the utilization of the first-principles techniques has been attempted: mixed-space cluster expansion,[1] the cluster variation method,[2,3] and further combination of atomic-level simulations with continuum theory.[4] These techniques are applied to large precipitates rather than the nucleus, and require the cluster expansion or other effective interaction extracted from the first-principles' results.

Recently, a treatment of the nucleation free energy calculation in alloy systems was proposed by Seko *et al.*[5] This technique directly applied the first-principles calculation to Fe-Cu binary and Ni-doped Fe-Cu ternary alloys. The most advantageous point in this treatment is the elimination of the ambiguity of the interface energy in the classical treatment. The static contribution to the enthalpy change and the configurational entropy change for cluster formation are accurately estimated, while the effect of lattice vibrations on the free energy change is neglected in the treatment. On the contrary, the importance of vibrational effects on phase stability have been actively examined both experimentally[6–9] and theoretically.[10–13] For the Al$_2$Cu system, the vibrational entropy contribution is shown to be essential in reversing the stability of θ and θ' phases.[13]

In order to investigate the vibrational effects on the nucleation free energy for Cu precipitates in the Fe-Cu system, the quasi-harmonic (QH) treatment[14,15] has been applied;[16] vibrational effects have been considered negligible under the assumption that the bond stiffness of unlike-atom pairs is equal to the arithmetic mean of those of like-atom pairs. Using the interatomic force constants, the model calculation of the vibrational contribution to nucleation was examined in terms of the interatomic force constants.[17] This study revealed that the effect of lattice vibration on nucleation free energy can be drastic and the above assumption of bond

stiffness for unlike-atom pairs can yield incorrect estimations. Therefore, in order to confirm how the lattice vibration affects the nucleation free energy, further investigation avoiding such assumptions should be performed.

In the present study, we first rewrite the expression of nucleation free energy change, which allows for the inclusion of the effects of lattice vibration. The thermal expansion effect induced by lattice vibration is also examined, and finally, the effects of lattice vibration on Cu nucleation free energy in the Fe-Cu system are quantitatively investigated by utilizing the first-principles techniques.

II. METHODOLOGY

A. Basic idea of calculational treatment

1. Nucleation free energy

We show schematic illustrations of the initial and final states describing the Cu nucleation process in the Fe-Cu system in Fig. 1. As shown, changes in cluster energy are calculated from the total energy changes between the initial states described as the sum of the isolated solute atoms, corresponding to the dilution limit, and the final state of the n-size Cu cluster.
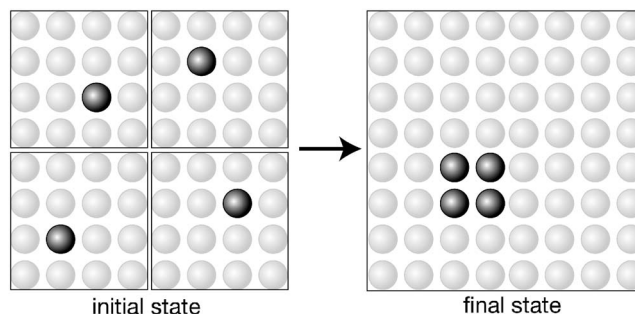

FIG. 1. Schematic illustration of the nucleation process. Gray spheres represent the solvent Fe atoms, and black ones the solute Cu atoms.

Including the vibrational contributions, the total nucleation free energy change ΔF_{tot} can be divided into the following three terms:

$$\Delta F_{\text{tot}} = \Delta F_{\text{config}} + \Delta F_{\text{vib}} + \Delta F_{\text{expand}}. \qquad (1)$$

The first term, ΔF_{config}, is the configurational free energy change for a rigid lattice. The second term represents the vibrational free energy change in equilibrium volume V_0 at temperature $T=0$ K, and the third the free energy change due to thermal expansion induced by lattice vibration. The vibrational contributions of ΔF_{vib} and ΔF_{expand} can be calculated from the vibrational free energy differences between initial and final states of Fig. 1, whose treatment are discussed in detail in Sec. III.

In the classical treatment, the effect of lattice vibration is typically neglected, and the free energy change is described by the sum of the negative driving force ΔF_{v} and the positive interface energy H_{s}, namely,

$$\Delta F_{\text{config}} = \Delta F_{\text{v}} + H_{\text{s}}. \qquad (2)$$

The main ambiguities in this treatment are the two assumptions that (i) the interface energy for a bulk cluster can be applied to a small precipitated cluster and (ii) the interface energy is isotropic. These problems can be successfully solved by using the following modification of the nucleation treatment.[5] The driving force, ΔF_{v}, is divided into two components of enthalpy change ΔH_{v} and entropy change $-T\Delta S_{\text{config}}$. Therefore Eq. (2) can be rewritten as

$$\Delta F_{\text{config}} = \left(\Delta H_{\text{v}} + H_{\text{s}}\right) - T\Delta S_{\text{config}}. \qquad (3)$$

The first term, $\Delta H_{\text{v}}(n) + H_{\text{s}}(n)$, which is called the cluster energy change including both enthalpy change for the cluster from isolated atoms and interface energy, can be directly obtained through the first-principles calculation; the interface energy between cluster and matrix is automatically included in this procedure. The second term of Eq. (3) mainly represents entropy loss due to cluster formation. This term is estimated within the Bragg-Williams approximation (see Appendix A) as

$$\Delta S_{\text{config}}(n) = k_{\text{B}}\left\{(n-1)\ln x - n + \frac{3}{2}\ln n + \frac{1}{2}\ln(2\pi)\right\}, \qquad (4)$$

where k_{B} represents the Boltzmann constant, x the initial solute concentration, and n the number of atoms in the precipitate cluster. We employ the above procedure to estimate the configurational part, ΔF_{config}.

2. Vibrational free energy

The vibrational free energies in the defect lattices are well treated by the effective medium approximation in the real-space calculation. The general expression of eigenequations for the lattice vibration within the harmonic approximation is given by

$$\boldsymbol{D} \cdot \boldsymbol{B} = \omega^2 \boldsymbol{B}, \qquad (5)$$

where ω denotes the angular frequency of the harmonic oscillator, and $\boldsymbol{B}$ the polarization vector. $\boldsymbol{D}$ is the $3N \times 3N$ (N is

the number of atoms in the system) dynamical matrix described as

$$\boldsymbol{D} = \boldsymbol{M}^{-(1/2)}\boldsymbol{\Phi}\boldsymbol{M}^{-(1/2)}, \qquad (6)$$

where $\boldsymbol{M}$ is the atomic mass tensor and $\boldsymbol{\Phi}$ is the interatomic force constant matrix. For a crystal, determination of the eigenstates of Eq. (5) is considerably simplified by the translational symmetry of the system. Let l denote the number of atoms per unit cell and k denote a point in the first Brillouin zone; then the problem of diagonalizing the $3N \times 3N$ matrix $\boldsymbol{D}$ is reduced to the problem of diagonalizing the $3l \times 3l$ matrix $\boldsymbol{D}(k)$.[18] This operation, the root-sampling method, is typically used to obtain the vibrational density of states (VDOS) and associated thermodynamic properties such as vibrational free energy.[19–22]

Other techniques to calculate the vibrational free energy have been developed in order to alleviate the diagonalization of dynamical matrix: (i) describing vibrational free energy F_{vib} in terms of the determinant of dynamical matrix, which provides a good approximation for exact values,[23] and (ii) local harmonic approximation[24] which models the VDOS as δ functions in terms of the second moment of VDOS. The latter approach reduces $3N \times 3N$ to $N(3 \times 3)$ diagonalization by neglecting off-diagonal 3×3 block matrices, and provides a reasonable agreement with QH approximation.[25] Another approach based on the second moment assumes the functional form for VDOS, which has been proposed by Sutton.[26] These techniques, which assume different form of VDOS, result in a different vibrational free energy itself; however, these differences typically cancel out for defect energy calculation.[25] In the supercell calculation, we only use diagonal elements of the dynamical matrix to estimate vibrational free energy, since an accurate estimation of the off-diagonal element of the dynamical matrix requires a much bigger supercell.[27] Therefore, latter approaches based on the second moment would be rather compatible with our calculation.

In the present article, we employ the effective medium approximation of the second moment expansion of Green's function, which have an explicit functional form of VDOS. The VDOS in this approximation is given by (see Appendix B)

$$g_{j\alpha}(\omega^2) = \frac{2}{\pi\left(\mu_{j\alpha}^{(1)}\right)^2}\left[\left(\mu_{j\alpha}^{(1)}\right)^2 - \left(\omega^2 - \mu_{j\alpha}^{(1)}\right)^2\right]^{1/2}, \qquad (7)$$

where j denotes the atom site, α the Cartesian coordinates, and $\mu_{j\alpha}^{(1)}$ equals the diagonal element $\boldsymbol{D}_{j\alpha j\alpha}$. The form of VDOS in Eq. (7) is quite similar to that of Sutton,[26] where we treats VDOS on mode basis, while Sutton treats per atom. Note that (i) Eq. (7) satisfies that VDOS is proportional to ω^2 at lower band edge, which is a desirable behavior of real DOS, and (ii) $g_{j\alpha}(\omega^2)$ has a bandwidth of $2\mu_{j\alpha}^{(1)}$ despite using only the diagonal element. In this description of VDOS, vibrational free energy $F_{j\alpha}$ becomes
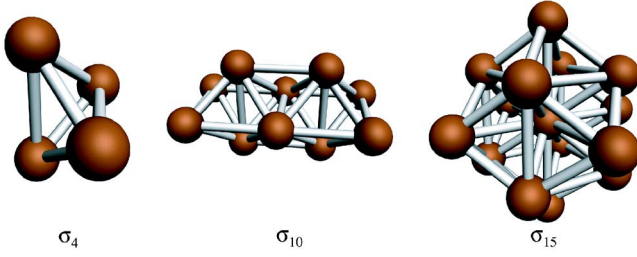
σ_4 σ_{10} σ_{15}

FIG. 2. (Color online) Atomic configurations for the Cu precipitate clusters.

$$F_{j\alpha} = k_{\rm B}T \int_0^{\infty} 2\omega g_{j\alpha}(\omega^2) \ln\left[2 \sinh\left(\frac{\hbar\omega}{2k_{\rm B}T}\right)\right] d\omega,$$

$$= \frac{16 k_{\rm B}T}{\pi} \int_0^1 y^2 (1-y^2)^{1/2} \ln\left[2 \sinh\left(\frac{c_{j\alpha} y}{2}\right)\right] dy, \quad (8)$$

where

$$c_{j\alpha} = \frac{\hbar (2\mu_{j\alpha}^{(1)})^{1/2}}{k_B T}, \quad y = \frac{\omega}{(2\mu_{j\alpha}^{(1)})^{1/2}}. \quad (9)$$

In order to assess the applicability of this approximation, we have compared the vibrational free energy of bcc-Fe at lattice parameter $a=2.813$, 2.833, and 2.853 Å, using an effective medium approximation with that using more accurate approximation, the root-sampling method; the free energy differences between two approximations are always ~ 4 (meV/atom) at $T=773$ K, which indicates that the effective medium approximation provides reasonable description of vibrational free energy. The above error would become rather small in the nucleation free energy calculation due to cancellation of errors when taking energy differences.

B. Computational details

The spin-polarized calculations were carried out using the Vienna *Ab initio* Simulation Package (VASP)[28,29] code. The interaction between the ions and valence electrons was described by a projector augmented-wave (PAW) method.[30,31] A plane-wave basis set with a cutoff of 290 eV was used. Sums over occupied electronic states are performed on Monkhorst and Pack's scheme,[32] on a $2\times2\times2$ set of the **k**-point mesh. To deal with the possible convergence problems for metals, the Methfessel-Paxton scheme[33] with the smearing parameter σ set to 0.2 was used. The exchange-correlation functional was described by the generalized gradient approximation (GGA) of the Perdew-Wang91 form.[34] The cluster energy has been calculated with 128 atoms ($4\times4\times4$ unit cells) under the structure relaxation condition. The calculated equilibrium lattice constants of bcc ferromagnetic Fe and bcc Cu are 2.833 Å and 2.880 Å, respectively. Cluster models were constructed by replacing some Fe sites with Cu atoms. Seko *et al.* determined the configurations of the Cu precipitate clusters, each of which has the minimum energy among all possible configurations.[5] Following their work, we construct supercells including specific Cu cluster configurations σ_4, σ_{10}, and σ_{15}, as shown in Fig. 2, where the

subscript represents the number of Cu atoms in the cluster.

The contribution to the vibrational free energy from specific atoms is obtained using Eq. (8). The diagonal elements of dynamical matrix $\mathbf{D}_{i\alpha i\alpha}$ are determined by the direct method.[35] First, we moved a chosen atom i from its equilibrium position along direction α by amplitude of 0.028 Å; then the corresponding Hellman-Feynman force[36] is estimated through first-principles calculation. For one direction α, atom i should be moved both in the positive and negative directions, then the Hellman-Feynman forces are arithmetically averaged in order to diminish the third-order anharmonic effects. Thus we can obtain the diagonal element $D_{i\alpha i\alpha}$ within the harmonic approximation and corresponding vibrational contribution to the free energy $F_{i\alpha}$.

III. RESULTS AND DISCUSSION

A. Thermal expansion effects on Cu nucleation free energy change

The vibrational motion induces thermal expansion, which affects the static energy and the free energy determined by the interatomic forces at slightly expanded volume. Thus substantial calculational effort is required to obtain the precise value of the free energy. However, a few simple assumptions lead to reasonably reliable estimation of the thermal expansion effect on the free energy.[18] Here, we will examine the volume dependence of the free energy at a specific temperature. The contribution of thermal expansion to the free energy, $F_{\rm therm}$, in equilibrium volume V at finite temperature T can be formally divided into

$$F_{\rm therm}(V) = \Delta E_{\rm stat}^{\rm therm}(V) + \Delta F_{\rm vib}^{\rm therm}(V)$$

$$= \{E_{\rm stat}(V) - E_{\rm stat}(V_0)\} + \{F_{\rm vib}(V) - F_{\rm vib}(V_0)\}, \quad (10)$$

where V_0 denotes the equilibrium volume at $T=0$ K, and $\Delta E_{\rm stat}^{\rm therm}(V)$ and $\Delta F_{\rm vib}^{\rm therm}(V)$ are the static and vibrational contributions to the free energy due to thermal expansion, respectively. We make two simple assumptions. (i) The changes in static energy are quadratic in volume as follows:

$$\Delta E_{\rm stat}^{\rm therm}(V) = \frac{B_0}{2V_0}(\Delta V)^2, \quad (11)$$

where B_0 is the bulk modulus at volume V_0 and $\Delta V = V - V_0$. (ii) For the volume dependence of the vibrational free energy, only the linear term is considered. Applying these two assumptions, we can rewrite Eq. (10) as

$$F_{\rm therm}(V) = \frac{B_0}{2V_0}(\Delta V)^2 + \frac{\partial F_{\rm vib}}{\partial V}\bigg|_{V=V_0} \Delta V. \quad (12)$$

The solution of minimizing Eq. (12) with respect to ΔV yields

$$\Delta V = -\frac{V_0}{B_0} \frac{\partial F_{\rm vib}}{\partial V}\bigg|_{V=V_0}. \quad (13)$$

By substituting Eq. (13) into Eq. (12), the contribution of thermal expansion to the free energy is finally given by

TABLE I. Calculated bulk modulus B_0, equilibrium volume V_0, and static energy change $\Delta E_{\text{stat}}^{\text{therm}}$ for specific configurations σ_i.

	B_0 (meV/Å^3)	V_0 (Å^3)	$\Delta E_{\text{stat}}^{\text{therm}}$ (meV)
σ_0	1170	1453.1	490
σ_1	1153	1454.9	483
σ_4	1062	1460.3	447
σ_{10}	985	1470.2	417
σ_{15}	958	1472.6	406

$$F_{\text{therm}}(V) = -\frac{1}{2}\frac{V_0}{B_0}\left(\left.\frac{\partial F_{\text{vib}}}{\partial V}\right|_{V=V_0}\right)^2. \quad (14)$$

The last term in Eq. (14) is identical to the negative of $\Delta E_{\text{stat}}^{\text{therm}}$ in Eq. (11). Thus it results in the surprising revelation that the thermal expansion effects on the free energy can be described only by the negative value of the static energy change.

In order to apply this derivation to Cu nucleation free energy, we assume that the linear thermal expansions of Fe-Cu cluster models are identical to those of bulk bcc-Fe due to the coherency of the precipitated Cu cluster with matrix. At 773 K, the volume thermal expansion $\Delta V/V_0$ is estimated to be 2.4% from our previous first-principles prediction.[16]

Table I shows the bulk modulus B_0, equilibrium volume V_0, and static energy change $\Delta E_{\text{stat}}^{\text{therm}}$ calculated for specific configurations σ_i using Eq. (11). Thermal expansion effects on nucleation free energy change, $\Delta F_{\text{expand}} = -\Delta E_{\text{stat}}^{\text{therm}}$, then can be given by the changes in energy measured from the dilution limit, namely,

$$\Delta F_{\text{expand}}(\sigma_n) = -[\Delta E_{\text{stat}}^{\text{therm}}(\sigma_n) - \Delta E_{\text{stat}}^{\text{therm}}(\sigma_0)]$$
$$+ n[\Delta E_{\text{stat}}^{\text{therm}}(\sigma_1) - \Delta E_{\text{stat}}^{\text{therm}}(\sigma_0)]. \quad (15)$$

Table II shows the contribution ΔF_{expand} for specific configurations σ_i. ΔF_{expand} is negligible in Cu nucleation free energy, which will be discussed in the following discussion.

B. Rough estimation of vibrational effects on nucleation free energy change

In order to investigate the vibrational effect ΔF_{vib} of Eq. (1) on Cu nucleation intuitively, we first assume that the interatomic scalar force constants are simply represented by

TABLE II. Calculated thermal expansion effects on Cu nucleation free energy ΔF_{expand} for specific configurations σ_i.

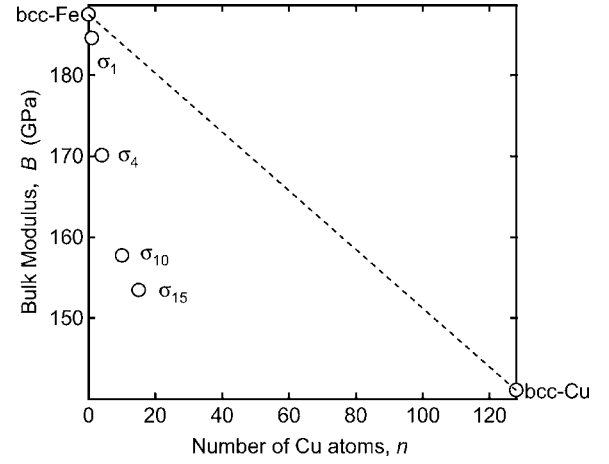|	ΔF_{expand} (meV)
σ_4	16
σ_{10}	6
σ_{15}	−17

FIG. 3. Calculated bulk modulus for configurations σ_i as a function of number of Cu atoms n in a supercell of 128 atomic sites.

the nearest neighbor atomic species, i.e., in the *A-B* binary system, there exist three kinds of force constants, k_{AA}, k_{BB}, and k_{AB}. This simplification implies that force constants and associated vibrational free energy depend only on the configuration of atoms, but not on the distance; we call this dependence the "configuration-dependent" vibrational effects. For configuration-dependent vibrational effects, we revealed a reasonable relationship between vibrational free energy change due to nucleation, ΔF_{vib}, and interatomic scalar force constants in our previous study;[17] ΔF_{vib} should be approximately cancelled when k_{AB} equals $(k_{AA}+k_{BB})/2$.

In the Fe-Cu system, the relationship among interatomic force constants is examined using bulk modulus B for configurations σ_i, obtained through first-principles calculation, as shown in Fig. 3. The broken line corresponds to $k_{AB} = (k_{AA}+k_{BB})/2$. For the Fe-Cu system, the interatomic spring constants satisfy

$$k_{\text{FeCu}} < \frac{k_{\text{FeFe}} + k_{\text{CuCu}}}{2}. \quad (16)$$

This relationship straightforwardly indicates that lattice vibration increases the Cu nucleation free energy change in the Fe-Cu system; in the process of Cu nucleation, the number of softer bonds between Fe and Cu, k_{FeCu}, rather than $(k_{\text{FeFe}}+k_{\text{CuCu}})/2$, decreases due to the clustering of solute Cu atoms. Thus within the configuration-dependent vibrational effects, Cu nucleation free energy is increased by lattice vibration.

C. Precise estimation of vibrational effects

Second, we proceed to a more quantitative estimation of the vibrational effects via the first-principles technique. We have calculated the vibrational free energy F_{vib} of all the atoms, including inside the Cu cluster, the interface between cluster and matrix, and the Fe matrix, for each configuration σ_i at $T=773$ K according to the procedure of Sec. II B (see Fig. 4). Note that F_{vib} for atoms located at the boundary between supercells have not been calculated, because during the structure optimization, relaxation of atoms on periodic
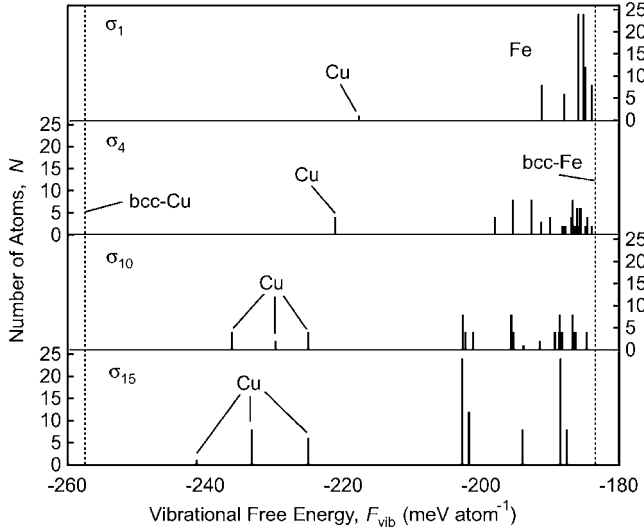
FIG. 4. Distribution of the vibrational free energy F_{vib} per atom for configurations σ_i.

FIG. 5. Total free energy change ΔF_{tot} of Cu precipitate nucleation in Fe-Cu system at $T=773$ K and the Cu concentration of 0.014. To see the impact of lattice vibration, the purely configurational contribution ΔF_{config} of Eq. (3) is also shown.

boundary are constrained by the symmetry: F_{vib} for these atoms should thus be omitted when taking vibrational free energy differences. The total vibrational free energy of a system in configuration σ_i is thus given by the sum of the vibrational contribution to the free energy from each atom.

The vibrational contribution to the nucleation free energy can be estimated in a similar way of evaluating ΔF_{expand} of Eq. (15) by the vibrational free energy of the final state measured from the dilution limit which corresponds to the initial states illustrated in Fig. 1, namely,

$$\Delta F_{vib}(\sigma_n, T) = [F_{vib}(\sigma_n, T) - F_{vib}(\sigma_0, T)] - n[F_{vib}(\sigma_1, T) - F_{vib}(\sigma_0, T)]. \quad (17)$$

The static contribution $\Delta H = \Delta H_v + H_s$ can be estimated in the same way, namely

$$\Delta H(\sigma_n, T) = [H(\sigma_n, T) - H(\sigma_0, T)] - n[H(\sigma_1, T) - H(\sigma_0, T)]. \quad (18)$$

Thus we can obtain the total free energy change due to nucleation, ΔF_{tot}, from the sum of the static contribution $\Delta H_v + H_s$, the vibrational contribution ΔF_{vib}, and the configurational entropy change $-T\Delta S_{config}$, as shown in Fig. 5. The entropy change is estimated at the temperature of 773 K and the concentration of 0.014 Cu, for comparison with the previous experimental results.[37,38] In order to interpret our results within the classical treatment, we assumed the interface energy to be constant and isotropic. Under this assumption, the cluster energy changes with and without vibrational free energy are, respectively, described by

$$\Delta H + H_s = an + bn^{2/3}, \quad (19)$$

$$\Delta H + H_s + \Delta F_{vib} = a'n + b'n^{2/3}. \quad (20)$$

The first term of the right-hand sides of Eqs. (19) and (20) represents the driving force without configurational entropy, and correspond to the dilution limit measured from the average static energy H_{ave} and that from the average vibrational
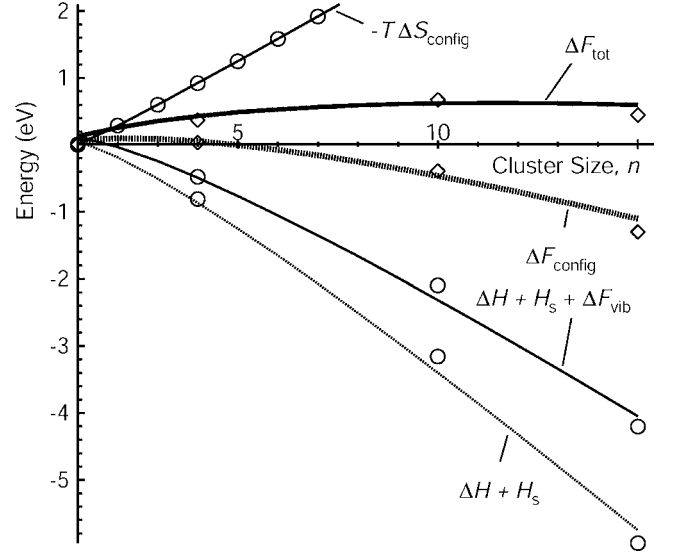
free energy F_{ave}^{vib}, respectively. Here, H_{ave} and F_{ave}^{vib} are defined as the line segment between the static and vibrational free energy for pure bcc-Fe and that for pure bcc-Cu, respectively. Coefficients a and a' are explicitly given by

$$-a = H(\sigma_1, T) - H_{ave}(n=1, T), \quad (21)$$

$$-a' = \{H(\sigma_1, T) + F_{vib}(\sigma_1, T)\} - \{H_{ave}(n=1, T) + F_{vib}^{ave}(n=1, T)\}. \quad (22)$$

The latter terms on the right-hand sides of Eqs. (21) and (22) correspond to the segregation limit of enthalpy and free energy at $n=1$ respectively. The second terms b and b' are fitting parameters for ΔF_{config} and ΔF_{tot}, and can be related to the interface energy, namely,

$$-b = H_s(3V)^{2/3}(4\pi)^{1/3}, \quad (23)$$

$$-b' = (H_s + \Delta F_{vib}^s)(3V)^{2/3}(4\pi)^{1/3}, \quad (24)$$

where V is the volume which one atom occupies in the cell, and ΔF_{vib}^s represents the vibrational contribution to the interface energy. We should restate one important point here that the lattice vibration contributes both to the driving force and the interface energy through Eqs. (22) and (24), respectively.

Table III shows the calculated static, vibrational, and configurational entropy contribution. It is obvious that the vibrational contribution ΔF_{vib} is comparable ($\sim 36\%$) to the configurational entropy term $-T\Delta S_{config}$, which cannot be neglected in the nucleation free energy change, as clearly seen in Fig. 5. On the contrary, the thermal expansion contribution ΔF_{expand} shown in Table II is proved to be negligible in the Cu nucleation free energy.

Table IV shows the calculated activation free energy, critical number, driving force without configurational entropy obtained through Eqs. (21) and (22), and interface energy

TABLE III. Calculated static, vibrational, and configurational entropy contributions for specific configurations σ_i. The unit for energy is eV.

	$\Delta H + H_\sigma$	ΔF_{vib}	$-T\Delta S_{config}$
σ_4	−0.81	0.33	0.92
σ_{10}	−3.16	1.06	2.93
σ_{15}	−5.94	1.74	4.65

obtained through Eqs. (23) and (24). The resulting activation barrier of Cu nucleation is estimated to be 0.62 eV at critical number n^* of 12, which is in satisfactory agreement with the experimentally predicted diameter $d \leqslant 10$ Å.[37,38] The inclusion of vibrational effects explicitly increases the activation barrier of Cu nucleation ΔF^* by 0.53 eV. Within the classical treatment, this can be interpreted in terms of the driving force F_D, rather than the interface energy, decreased by lattice vibration, as shown in Table IV, being the dominant contribution to the increase of the activation barrier of Cu nucleation.

IV. CONCLUSIONS

We have investigated the vibrational contribution to the Cu nucleation free energy in the Fe-Cu system. When the dependence of the thermal expansion of a precipitated bcc Cu cluster on temperature is assumed to be identical to that of matrix bcc Fe, the thermal expansion effect of static and vibrational contributions to Cu nucleation free energy is negligible under a simple anharmonic model. This allows the total free energy change to be calculated at finite temperature T, and, in the equilibrium lattice volume V_0, at $T=0$. The utilization of the effective medium approximation with the first-principles technique reveals that the vibrational effect is comparable ($\sim 36\%$) to the configurational entropy, which increases the activation barrier of Cu nucleation by 0.53 eV. In the Fe-Cu system, this increase can also be predicted by applying our previous model of lattice vibration to the fact that the number of softer bonds between Fe and Cu, k_{FeCu}, rather than $(k_{FeFe} + k_{CuCu})/2$, should decrease due to the clustering of solute Cu. We estimated the activation barrier ΔF^* to be 0.62 eV at critical number n^* of 12, which is in satisfactory agreement with the experimental prediction.

APPENDIX A

The configurational entropy expression of Eq. (4) due to precipitate nucleation is derived from the Bragg-Williams

TABLE IV. Calculated activation free energy ΔF^*, critical number n^*, driving force without configurational entropy F_D, and interface energy F_s using ΔF_{config} (no vib) and ΔF_{tot} (with vib).

	ΔF^* (eV)	n^*	F_D (eV/atom)	F_s (J/m²)
ΔF_{config}	0.09	2	−0.68	0.49
ΔF_{tot}	0.62	12	−0.53	0.43

approximation applying the initial and final states, as illustrated in Fig. 1. Let n denote the cluster size and x the concentration of the solute. We define the size of the system M as

$$M = n/x. \quad (A1)$$

Therefore, the number of arrangements in the initial states is

$$W_{initial} = \frac{M!}{(Mx_{Cu})! \, [M(1-x_{Cu})]!}. \quad (A2)$$

For the final states, when rotation of the cluster is neglected and only the translation is taken into account, the number of arrangements is given by

$$W_{final} = M \quad (A3)$$

because of the periodic boundary condition. Therefore, within the Bragg-Williams approximation, configurational entropy change due to nucleation becomes

$$\frac{\Delta S_{config}}{k_B} = \ln \frac{(Mx)! \, [M(1-x_{Cu})]!}{(M-1)!}. \quad (A4)$$

Finally, applying Stirling's formula and Taylor expansion around $x=0$ to Eq. (A4), we obtain Eq. (4).

APPENDIX B

The effective medium approximation of the second-order moment expression of Eq. (7) is derived. The phonon local density of states (LDOS) at atom j is first written as

$$n_{j\alpha}(\omega) = -\frac{2\omega}{\pi} Im \, G_{j\alpha j\alpha}(\omega^2 + i0)$$

$$= -\frac{2\omega}{\pi} \lim_{\epsilon \to 0} Im \langle \alpha, j | \frac{1}{(\omega^2 + i\epsilon)I - D} | \alpha, j \rangle, \quad (B1)$$

where α represents the direction; the Green's function $G_{j\alpha j\alpha}(\omega^2 + i0)$ is the resolvent operator $[\omega^2 I - D]^{-1}$; I is the unit matrix; and $|\alpha, j\rangle$ is the corresponding vibrational state vector. Green's function $G_{j\alpha j\alpha}$ can be expanded as a continued fraction

$$G_{j\alpha j\alpha}(\omega^2) = \cfrac{1}{\omega^2 - a_0 - \cfrac{b_1^2}{\omega^2 - a_1 - \cfrac{b_2^2}{\omega^2 - a_2 - \cdots}}}, \quad (B2)$$

where coefficients $\{a_n\}$ and $\{b_n\}$ are determined from the orthonormality property of the new basis with starting vector $|\alpha, j\rangle$. This scheme, the "excursion method,"[39,40] has been applied to the calculations of the electronic and vibrational DOS of surface and amorphous materials.[41] In terms of the moment of lattice vibration, truncating the expansion of Eq. (B2) up to level n corresponds to including the first $2n$ moments. For instance, let $|0\rangle$ denote the normalized starting state $|\alpha, j\rangle$, and $|1\rangle$ the next state interacting with the

previous state. Then the first coefficients a_0 and b_1 satisfy the following recursion relation:

$$a_0 = \langle 0|\boldsymbol{D}|0\rangle,$$

$$b_1 = \langle 1|\boldsymbol{D}|0\rangle. \tag{B3}$$

Therefore, the associated second-order moment of matrix $\boldsymbol{D}$ becomes

$$\mu_{j\alpha}^{(2)} = \langle 0|\boldsymbol{D}|0\rangle^2 + \langle 0|\boldsymbol{D}|1\rangle\langle 1|\boldsymbol{D}|0\rangle = a_0^2 + b_1^2. \tag{B4}$$

In the present study, we will expand Green's function $G_{j\alpha j\alpha}(\omega^2)$ to the first order and then terminate, namely,

$$G_{j\alpha j\alpha}(\omega^2) = \frac{1}{\omega^2 - a - b^2 G_{j\alpha j\alpha}(\omega^2)}. \tag{B5}$$

This is the effective medium approximation of the second-order moment expansion of Eq. (B2). Substituting Green's function of Eq. (B5) into Eq. (B1) naturally leads to the semielliptic form of the local density of states, whose center of gravity and bandwidth are specified by coefficients a and b, respectively.

Coefficient a is identical to the first moment $\mu_{j\alpha}^{(1)} = \langle 0|\boldsymbol{D}|0\rangle$. For a harmonic crystal, the dynamical matrix $\boldsymbol{D}$ should have positive eigenvalues and three zero eigenvalues at Γ-point associated with a rigid translation of a system. When we determine coefficient b such that the minimum vibrational frequency of LDOS equals zero, the expression of LDOS becomes $g_{j\alpha}(\omega^2)$ of Eq. (7).

---

[1] C. Wolverton, V. Ozolins, and A. Zunger, Phys. Rev. B **57**, 4332 (1998).

[2] M. Sluiter and Y. Kawazoe, Phys. Rev. B **54**, 10381 (1996).

[3] M. Asta and J. J. Hoyt, Acta Mater. **48**, 1089 (2000).

[4] V. Vaithyanathan, C. Wolverton, and L. Q. Chen, Phys. Rev. Lett. **88**, 125503 (2002).

[5] A. Seko, S. R. Nishitani, I. Tanaka, H. Adachi, and E. F. Fujita, CALPHAD: Comput. Coupling Phase Diagrams Thermochem. **28**, 173 (2004).

[6] L. Anthony, J. K. Okamoto, and B. Fultz, Phys. Rev. Lett. **70**, 1128 (1993).

[7] L. Anthony, L. J. Nagel, J. K. Okamoto, and B. Fultz, Phys. Rev. Lett. **73**, 3034 (1994).

[8] B. Fultz, L. Anthony, L. J. Nagel, R. M. Nicklow, and S. Spooner, Phys. Rev. B **52**, 3315 (1995).

[9] B. Fultz, L. Anthony, J. L. Robertson, R. M. Nicklow, S. Spooner, and M. Mostoller, Phys. Rev. B **52**, 3280 (1995).

[10] G. D. Garbulsky and G. Ceder, Phys. Rev. B **53**, 8993 (1996).

[11] A. van de Walle, G. Ceder, and U. V. Waghmare, Phys. Rev. Lett. **80**, 4911 (1998).

[12] V. Ozolins, C. Wolverton, and A. Zunger, Phys. Rev. B **58**, R5897 (1998).

[13] C. Wolverton and V. Ozolins, Phys. Rev. Lett. **86**, 5518 (2001).

[14] A. A. Maradudin, E. W. Montroll, G. H. Weiss, and I. P. Ipatova, *Theory of Lattice Dynamics in the Harmonic Approximation*, 2nd ed. (Academic, New York, 1971).

[15] R. E. Allen and F. W. de Wette, Phys. Rev. **179**, 873 (1969).

[16] K. Yuge, A. Seko, K. Kobayashi, T. Tatsuoka, S. R. Nishitani, and H. Adachi, Mater. Trans., JIM **45**, 1473 (2004).

[17] K. Yuge, S. R. Nishitani, and I. Tanaka, CALPHAD: Comput. Coupling Phase Diagrams Thermochem. **28**, 167 (2004).

[18] A. van de Walle and G. Ceder, Rev. Mod. Phys. **74**, 11 (2002).

[19] S. M. Foiles and J. B. Adams, Phys. Rev. B **40**, 5909 (1989).

[20] J. D. Althoff, P. B. Allen, R. M. Wentzcovitch, and J. A. Moriarty, Phys. Rev. B **48**, 13253 (1993).

[21] S. Biernacki and M. Scheffler, Phys. Rev. Lett. **63**, 290 (1989).

[22] C. H. Xu, C. Z. Wang, C. T. Chan, and K. M. Ho, Phys. Rev. B **43**, 5024 (1991).

[23] J. R. Morris and K. M. Ho, Phys. Rev. Lett. **74**, 940 (1995).

[24] R. LeSar, R. Najafabadi, and D. J. Srolovitz, Phys. Rev. Lett. **63**, 624 (1989).

[25] S. M. Foiles, Phys. Rev. B **49**, 14930 (1994).

[26] A. P. Sutton, Philos. Mag. A **60**, 147 (1989).

[27] A. van de Walle, Ph.D. thesis, Massachusetts Institute of Technology, 2000.

[28] G. Kresse and J. Hafner, Phys. Rev. B **47**, R558 (1993).

[29] G. Kresse and J. Furthmüller, Phys. Rev. B **54**, 11169 (1996).

[30] G. Kresse and D. Joubert, Phys. Rev. B **59**, 1758 (1999).

[31] P. E. Blöchl, Phys. Rev. B **50**, 17953 (1994).

[32] H. J. Monkhorst and J. D. Pack, Phys. Rev. B **13**, 5188 (1976).

[33] M. Methfessel and A. T. Paxton, Phys. Rev. B **40**, 3616 (1989).

[34] J. P. Perdew and Y. Wang, Phys. Rev. B **45**, 13244 (1992).

[35] K. Parlinski, computer code PHONON (Krakow, Poland, 2002).

[36] R. P. Feynman, Phys. Rev. **56**, 340 (1939).

[37] S. R. Goodman, S. S. Brenner, and J. R. Low, Jr., Metall. Trans. **4**, 2363 (1973).

[38] S. R. Goodman, S. S. Brenner, and J. R. Low, Jr., Metall. Trans. **4**, 2371 (1973).

[39] R. Haydock, V. Heine, and M. Kelly, J. Phys. C **5**, 2845 (1972).

[40] R. Haydock, V. Heine, and M. Kelly, J. Phys. C **8**, 2591 (1975).

[41] P. E. Meek, Philos. Mag. **33**, 897 (1976).